JOURNAL OF MATERIALS SCIENCE 28 (1993) 5240–5246

Fracture mechanism in short fibre reinforced thermoplastic resin composites

G. M. LIN
Department of Physics, Zhongshan University, Guangzhou 510 275, China
J. K. L. LAI
Department of Applied Science, City Polytechnic of Hong Kong, Tat Chee Avenue, Kowloon, Hong Kong

The properties of two types of short carbon fibre (CF) reinforced thermoplastic resin composites (CF–PPS and CF–PES-C), such as strength (σ_y), Young's modulus (E) and fracture toughness (K_{1c}), have been determined for various volume fractions (V_f) of CF. The results show that the Young's modulus increases linearly with increasing V_f with a Krenchel efficiency factor of 0.05, whereas σ_y and K_{1c} increase at first and then peak at a volume fraction of about 0.25. The experimental results are explained using the characteristics of fibre–matrix adhesion deduced from the load–displacement curves and fractography. By using a crack pinning model, the effective crack tensions (T) have been calculated for both composites and they are 57 kJ m^{-1} for CF–PPS and 4.2 kJ m^{-1} for CF–PES-C. The results indicate that the main contribution to the crack extension originates from localized plastic deformation of the matrix adjacent to the fibre–matrix interface.

1. Introduction

The principal parameters determining the mechanical properties of resin-based composites are the volume fraction of the filler, which may be particulates or fibres, its particle size or fibre aspect ratio, its modulus and strength, the filler–matrix adhesive strength, and the toughness of the matrix [1–3].

Young [2–4] studied in detail the strengthening mechanisms in rigid-particulate (glass bead) reinforced thermosetting resin composites. He showed that the addition of rigid filler particles to thermosetting polymers did not necessarily lead to a deterioration in properties. In fact, it could often lead to an improvement in certain properties. The best property improvement was generally obtained with the use of bonding agents to provide good particle–matrix adhesion. The improvement in properties included better resistance to crack propagation compared with those without the use of bonding agents. The toughness of the composites could be improved further by adding a rubbery phase together with rigid particles in the matrix to produce a hybrid composite.

The study of the fracture behaviour of polymer composites is important because the practical applications of these materials are often limited by their toughness. The application of linear elastic fracture mechanics has led to some progress in the understanding of the fracture behaviour of these materials [4]. Usually, the value of the plane strain fracture toughness (K_{1c}) increases with increasing filler volume fraction (V_f). For poor filler–matrix adhesion a linear variation of K_{1c} versus V_f is observed, whereas a maximum K_{1c} occurs for good adhesion [1–3, 5]. The larger the particle size, the larger is the toughening effect. Because the Young's modulus E is very dependent on V_f in composites, it is better to use the rate of release of strain energy or fracture energy (G_{1c}) to describe the fracture behaviour of resin-based composites. G_{1c} may be related to K_{1c} by the equation.

$$G_{1c} = 2\gamma_p \simeq \frac{K_{1c}^2}{E} \quad (1)$$

where γ_p is the effective surface energy density.

Detailed reviews of the toughening mechanisms of particulate-filled composites have been published [1, 2, 3, 6]. Lange and Radford [7], Evans [8] and Green *et al.* [9] proposed and modified a crack pinning model to explain the toughening effect in particle-reinforced resin-based composites. The model is similar to the interaction between dislocations and dispersed particles in the plastic deformation of metals, which is known as the Orowan mechanism [10]. The interaction between the crack and the reinforced particles occurs during crack propagation in the case of good filler–matrix adhesion. Therefore, the hindered crack can only bow out between the well-bonded particles, forming secondary cracks and breaks away from pinning positions when it attains a radius $D/2$, where D is the interparticle spacing. The toughening effect depends on the interparticle spacing D and the effective crack line tension T, i.e. the line energy per unit length of the bowed crack front. The maximum toughening effect may be expressed as

$$G_{1c} = G_{1c}^m + \frac{2T}{D} \quad (2)$$

0022–2461

where G_{1c} and G_{1c}^{m} are the fracture energies of the composite and the matrix, respectively. The contribution to T originates from dissipation processes, for example debonding, local plastic deformation near the interface etc. Although these results have been obtained primarily from the study of spherical particle reinforced resin composites (for example, alumina trihydrate–epoxy [7] and glass–epoxy resin [6]), in principle they may be adequate to describe the behaviour of other types of composites filled by non-spherical particles [4]. Furthermore, Faber and Evans [11] showed that the crack pinning model is also adequate to be applied to randomly distributed rod-shaped particle (or short fibre) filled systems, provided that the effective interparticle spacing between the randomly arranged rod-shaped particles is available.

In the case of poor filler–matrix adhesion, another mechanism, i.e. crack tip blunting, is important [12]. Early debonding leads to blunting of the crack tip, by which the stress intensity factor K_1 near the crack tip will be reduced considerably. It has been observed in some composites with poor filler–matrix adhesion that the crack tends to propagate in an unstable stick–slip manner. When unstable propagation occurs, the load–deplacement curve has a characteristic sawtooth shape [2, 3]. It appears that the unstable stick–slip propagation is probably due to repeated crack initiations and arrests due to crack tip blunting.

There is no doubt that matrix toughness also plays an important role in determining the mechanical properties of polymer composites. Recently, Gupta *et al.* [13] studied the energy-absorbing mechanisms during fracture in polypropylene reinforced with short glass fibres. They suggested that the total work of fracture included contributions from the debonding of the interface, the sliding or pull-out of fibres, and the plastic deformation of the matrix. They reckoned that the contribution from matrix plasticity, either through homogeneous deformation of the matrix or from localized deformation around the fibre ends, was dominant.

The plastic deformation behaviour of thermoset resins is essentially identical to that of amorphous thermoplastics [14]. In practice, the controlling mechanism of fracture in polymer composites is determined by the strength, modulus and ductility of the filler and the matrix, and the filler–matrix adhesive strength. For example, Hine *et al.* [15] pointed out that for a ductile matrix a strong adhesive bond between the fibre and the matrix is important to enable stress to be transferred, thereby allowing substantial deformation of the matrix phase to take place. By contrast, for a brittle matrix, it is often better to have a weak fibre–matrix interface. The breaking of the interface increases the energy absorption by additional fibre pull-out and debonding.

In this paper, we measure the strength and fracture properties of two types of short fibre reinforced thermoplastic resin composite (SFRTP) as a function of carbon fibre (CF) volume fraction. The failure mode and fracture mechanism are specially considered. These results are compared with theoretical studies.

2. Experimental procedure

2.1. Preparation of composites

The materials used in this study were SFRTPs manufactured by the hot-pressing method. The filler fibre was high-strength grade PAN carbon fibre with a diameter of 7 cm and Young's modulus of 240 GPa. Before usage, the carbon fibres were burned in air for 0.5 h at a temperature of 400 °C to remove the glue layer. They were then cut into about 0.5 mm lengths in a high-speed cutting blender.

The matrices were two types of high-performance thermoplastic polymer: phenolphthalein side-group polyethersulphone (PES-C) and polyphenylene sulphide synthesized by sodium chloride treatment (PPS). Their glass transition temperatures were 260 and 90 °C respectively. PPS was cross-linked in air at a temperature of 270 °C for 6 h. The specific viscosity of PES-C was 0.68.

Samples with certain proportions of short CF and PES-C (or PPS) powder were completely mixed in industrial alcohol and then dried. Composites which contained various CF volume fractions were fabricated by hot-pressing in a mould at a temperature of 360 °C and a pressure of 70–80 MPa. The volume fractions of CF in our study were 0, 0.1, 0.25 and 0.4.

2.2. Determination of mechanical properties

2.2.1. Strength properties

The specimens for measuring the strength σ_y and Young's modulus E were rectangular in shape with dimensions of 70 mm × 12 mm × 6 mm and 70 mm × 15 min × 6 mm, respectively. σ_y was determined using uniaxial tensile tests at a tensile strain rate $\dot{\varepsilon}$ of $2 \times 10^{-4}\ s^{-1}$. Three-point bend tests were used to measure the Young's modulus, E. During the test, the load P versus displacement (Δ) curve was recorded directly by a high-sensitivity X–Y recorder. The descending rate of the crosshead was 0.5 mm min^{-1}. The value of E can be calculated from the formula [16]

$$E = \left(\frac{P}{\Delta}\right)\frac{l^3}{4bh^3} \tag{3}$$

where P/Δ is the initial slope of the loading curve, l is the span length of the test and b, h are the width and thickness of the specimen, respectively.

2.2.2. Fracture properties

The values of the fracture toughness were determined by three-point-bend tests. The thickness t and width w of the specimens used were 7 and 14 mm, respectively. The span length s was $4w$. A narrow notch of length 5 mm was produced with a razor blade. A crack tip of length 1.5–2.5 mm was then produced with a fine molybdenum wire (diameter $\phi \simeq 11$ μm) impregnated with 300 grade diamond paste. The resulting total initial length of the crack, a_0, was about (0.45–0.55)w. The experimental procedure and method of calculation conformed to ASTM standard E399(83). After testing, the fracture surfaces of the specimens were

coated with gold in a sputtering machine and examined in a Jeol JEM-820 scanning electron microscope (SEM).

All tests for determining mechanical properties were carried out at room temperature. Each result represents the average of at least two tests.

3. Results and discussion

3.1. Influence of CF volume fracture on strength and fracture properties

Figs 1 and 2 show respectively the variations of σ_y, E, K_{1c} and G_{1c} with V_f, the volume fractions of CF in CF–PES-C and CF–PPS composites. The modulus E varies as a linear function of V_f. This linear relationship can be described by the law of mixtures given below:

$$E = \eta E_f V_f + E_m V_m \quad (4)$$

where the subscripts f and m refer to the fibre and the matrix respectively and η is the Krenchel efficiency factor [17].

The value of η can be determined from the slopes of Fig. 1a and b. For both materials η is equal to 0.05. According to Folks [18], for short fibre reinforced systems the total efficiency factor may be written as $\eta = \eta_0\eta_l$, where η_0 is the efficiency factor of continuous fibres and η_l represents the effect of short fibres. From Krenchel [17], $\eta_0 = 1$ if the load is applied parallel to the fibre axis in the case of uniaxially aligned continuous fibres, and $\eta_0 = 0.2$ when the reinforcing fibres are randomly orientated in three dimensions. For our two SFRTP materials, with $\eta = 0.05$ and $\eta_0 = 0.2$, η_l is equal to 0.25.

η_l is dependent on the average fibre length l, the fibre orientation, and the fibre–matrix adhesive strength. Since both materials have the same average fibre length and orientation distribution, this result implies that the fibre–matrix adhesive strengths of both materials are the same. However, since the Young's modulus measurements are performed under static loading conditions, it is worth emphasizing that this similarity of fibre–matrix adhesive strengths of the two materials is valid under static conditions. This static adhesive bonding is the dominant factor in determining the transfer of elastic stresses and strains upon loading.

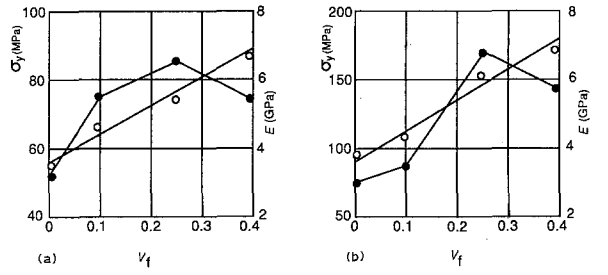

Figure 1 (●) Strength σ_y and (○) Young's modulus E versus CF volume fraction V_f in (a) CF–PES-C and (b) CF–PPS composites.

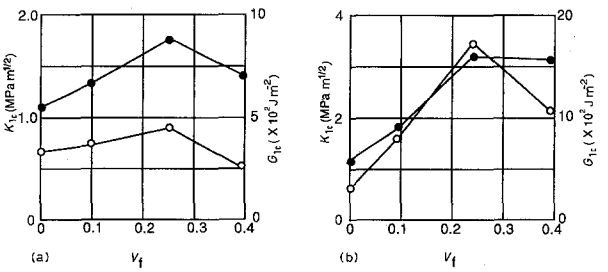

Figure 2 (●) Fracture toughness K_{1c} and (○) fracture energy G_{1c} versus CF volume fraction V_f in (a) CF–PES-C and (b) CF–PPS composites.

From Fig. 1, the strengths, σ_y of both materials vary with V_f and reach a maximum at $V_f = 0.25$. This result is similar to those obtained in short glass fibre reinforced thermoplastic resin composites [19]. The relationship between σ_y and V_f is complicated. Apart from the fibre orientation and the fibre–matrix adhesive strength, other factors such as stress concentrations at the fibre poles and the constraint on matrix deformation arising from the interaction of neighbouring fibres are also relevant. The fibre poles, where high stress concentrations are present when the material is loaded beyond the elastic region, are often the sites for the nucleation of microcracks [20, 21].

Since the strength of the fibres is much greater than that of the matrix, an increase in V_f is expected to lead to an increase in σ_y of the composite. However, an increase in V_f also leads to an increase in the number of nucleation sites for microcracks, which would have the opposite effect on σ_y. These two competing effects would lead to a maximum σ_y at an intermediate value of V_f as shown in Fig. 1.

Let us define the maximum effect of strengthening as $S = (\sigma_{max} - \sigma_0)/\sigma_0$, where σ_{max} is the maximum value of σ_y, and σ_0 is the value when $V_f = 0$. For the CF–PPS composite S reaches 1.31, which is larger than that of CF–PES-C, where S is only 0.68. Thus, although Young's modulus measurement shows that the fibre–matrix adhesive strengths are similar in the two materials studied under static loading conditions, the measurement of σ_y shows that the fibre–matrix adhesive strength in CF–PPS is stronger than that of CF–PES-C under dynamic loading conditions. The dynamic bonding strength is a critical parameter determining the transferability of plastic deformation through the fibre–matrix interface.

As shown in Fig. 2, K_{1c} and G_{1c} also exhibit peak values at about $V_f = 0.25$. The relationships of σ_y (strength) versus V_f and G_{1c} (toughness) versus V_f are very similar. This suggests that one mechanism is dominant at high values of V_f. That is to say, microcracking induced at fibre poles plays an important role at high values of V_f.

3.2. Comparison of fracture modes

Fig. 3 shows typical load–displacement (P–Δ) curves for the two materials. At zero or low V_f (i.e. $V_f = 0.1$), the loading curves are almost linear until the point of maximum load. But at high V_f (i.e. $V_f = 0.25$ or 0.40) the loading curves are not as linear. For $V_f = 0.25$ the knee of the loading curve (indicated by an arrow in Fig. 3), at which the P–Δ curve deviates from linearity,

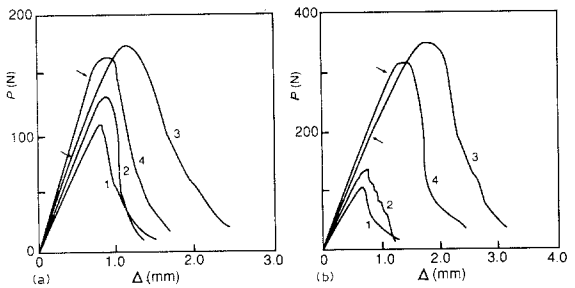

Figure 3 Typical load–displacement curves in three-point bend tests of (a) CF–PES-C and (b) CF–PPS composites: (1) pure matrix, (2) 10 vol % CF, (3) 25 vol % CF, (4) 40 vol % CF.

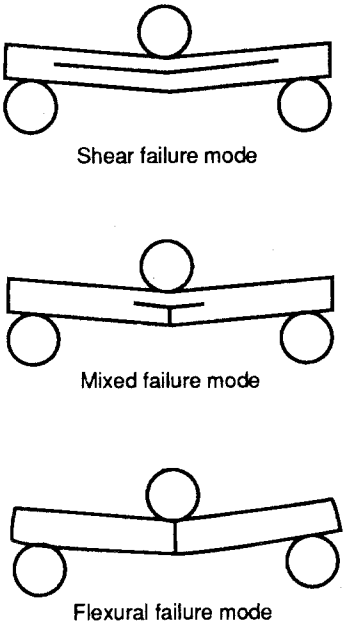

Figure 4 Schematic representations of three types of failure mode observed in three-point bend tests of polymer-matrix composites.

begins quite early. There is a relatively long period of non-linear stable crack propagation before the point of maximum load is reached. Furthermore, there is a long tail before final failure. For $V_f = 0.4$, the knee of the P–Δ curve at which deviation from linearity occurs is not far from the point of maximum load. The period of non-linear stable crack propagation is shorter than that of the material with $V_f = 0.25$.

It is likely that the knee in the P–Δ curve corresponds to the point of crack initiation in the material, and that the non-linear region between the knee and the point of maximum load corresponds to multiple cracking, giving rise to "pseudo-ductility" [20, 22, 23] which may reduce the notch (or crack) sensitivity, and improve the ductility of the composite.

According to the Bernoulli–Euler theory [16], when a long rectangular specimen is loaded in the three-point bend mode the maximum flexural stress, σ_{max} (tensile or compressive) and the maximum interlaminar shear stress, τ_{max}, exist at the surface of the specimen and at the neutral axis, respectively. The specimen can fail in a flexural mode at the surface or in a shear mode at the neutral axis, depending on whether σ_{max} or τ_{max} becomes critical. In practice, however, a mixed failure mode can also occur when the flexural and shear failures take place simultaneously. Schematic representation of these three failure modes are shown in Fig. 4.

Hanna and Steingiser [24] reported that failure modes can be deduced from the shape of the P–Δ curves of three-point bend tests. When a flexural failure occurs, the specimen fails abruptly at the point of maximum load, P_{max}, of the linear P–Δ curve. When a shear failure occurs, the slope of the P–Δ curve decreases gradually with increasing load after the point of crack initiation, and reaches a zero value constituting a characteristic plateau of the P–Δ curve before final failure. If the shape of the P–Δ curve is between these two extremes, the failure mode can be considered as mixed.

According to this criterion, pure matrix and low V_f (for example, $V_f = 0.1$) specimens of the two materials tested in this investigation fail in a flexural mode, as can be seen from the P–Δ curves in Fig. 3. On the other hand, high-V_f specimens fail in a mixed mode without exception. It is expected that, when the composite fails in a mixed mode, different micro-mechanisms, e.g. debonding of the interface, sliding and pull-out of carbon fibres, and cracking of the constrained matrix between carbon fibres, occur simultaneously. This is in agreement with the results of fractography described below.

3.3. Mechanism of toughening

The basic principle of increasing the toughness of resin-based composites lies in the introduction of various energy-absorbing processes such as filler (particulate or fibre) deformation, debonding of the interface, pull-out of fibres, homogeneous and localized plastic deformation of the matrix, and multiple cracking. Several theoretical models have been proposed, including crack pinning [7–9], crack blunting [12] and crack deflection [11].

The values of the fracture energy G_{1c} determined in this investigation are relatively low (less than $2\,kJ\,m^{-2}$) for all specimens tested, so the materials with which we are concerned are low-toughness composites and the contribution from the matrix to the toughness is small.

As can be seen from the fractographs of Fig. 5, "tails" were formed behind the carbon fibres as a result of the interaction between the propagating crack and the carbon fibres after the crack front had broken away from the latter. The fracture steps or river patterns formed by merging different fracture planes are visible, particularly in Fig. 5a. These can be considered a secondary cracking phenomenon [4]. Besides debonding of the interface and pull-out of carbon fibres, localized plastic deformation near the interface was observed, implying a certain degree of fibre–matrix adhesion in these materials.

The strength and Young's modulus of carbon fibres are much larger than those of the resin matrix. Thus, the carbon fibres can be considered as impenetrable "rigid fillers" during the fracture process. However, the carbon fibre–resin matrix bond strength is not large

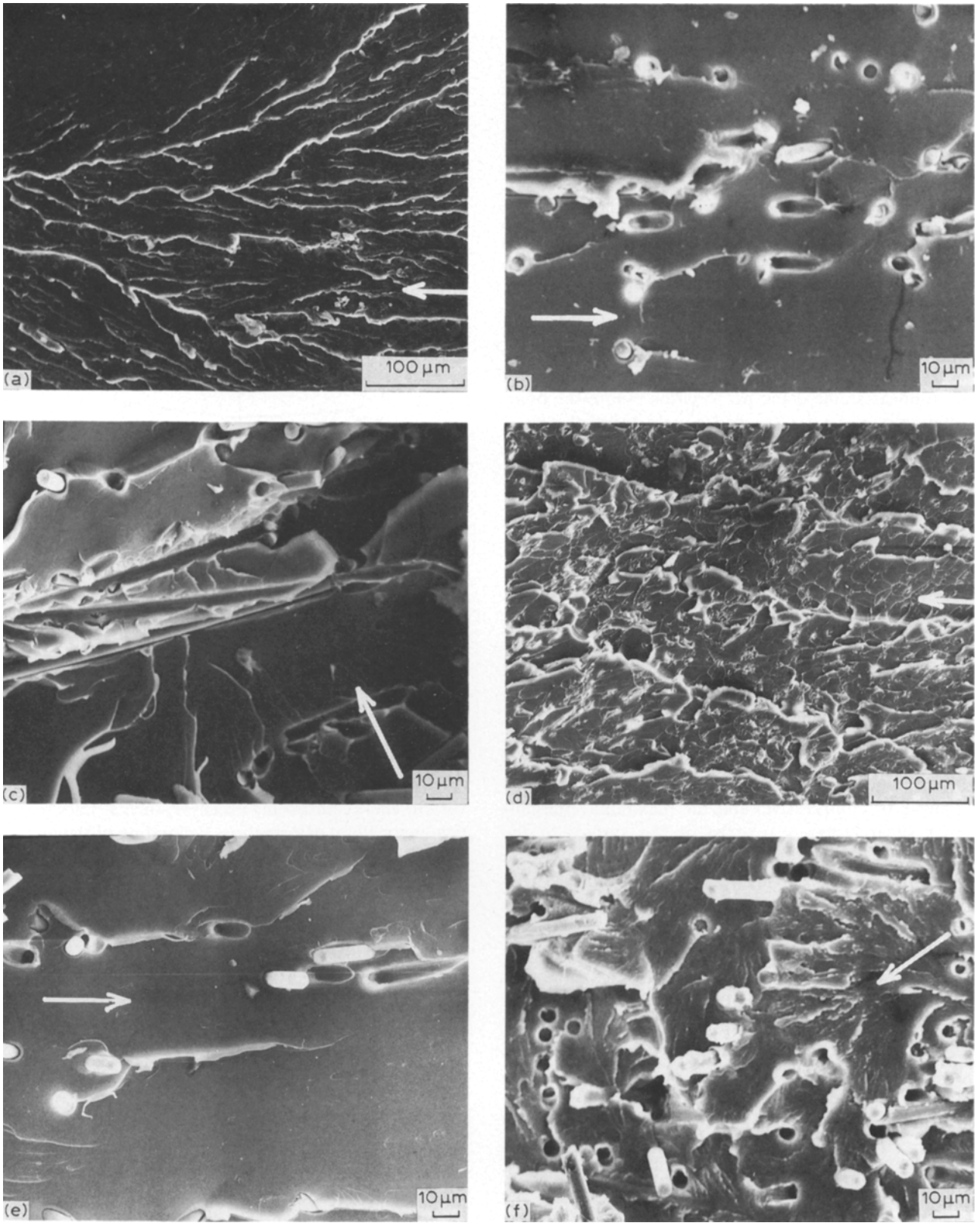

Figure 5 SEM fractographs of (a) PPS matrix, (b) 10 vol % CF–PPS, (c) 25 vol % CF–PPS, (d) PES-C matrix, (e) 10 vol % CF–PES-C, (f) 25 vol % CF–PES-C (crack propagation directions indicated by arrows).

due to the lack of chemical bonding, since the carbon fibres were not treated with special active agents [25].

As can be seen from the P–Δ curves in Fig. 3, unstable stick–slip crack propagation occurs in the CF–PPS composite with $V_f = 0.1$. This characteristic sawtooth shape is thought to be caused by crack-tip blunting in the case of poor fibre–matrix adhesion [2, 3]. Therefore, from the point of view of resistance to crack propagation, short carbon fibres are relatively weak obstacles resulting in a moderate toughening (see Fig. 2) [11].

From the above observations we believe that crack pinning is a major toughening mechanism in the two composite materials studied. The relationship between

the fracture energy G_{1c} and the effective carbon fibre spacing D is shown in Fig. 6 for the two materials studied. According to Equation 2, G_{1c} should be inversely proportional to D. For short carbon fibres, the value of D may be calculated from [26]

$$\frac{D}{d} \simeq \frac{e^{4V_f}}{V_f^{1/2}} \int_{4V_f}^{\infty} x^{1/2} e^{-x} dx \quad (5)$$

where d is the average diameter of the fibres.

As shown in Fig. 6, G_{1c} varies linearly with D^{-1} between $D^{-1} = 0$ to $D^{-1} \simeq 25\ mm^{-1}$. This result is similar to those reported in other crack pinning systems (e.g. [7]). In other words, the crack is "flexible" and the crack front bows out between the "CF particles", forming secondary cracks under the action of the driving force. Thus, energy is required not only to create the new fracture surface but also to be supplied to the newly formed non-linear crack front, resulting in an increase of G_{1c}. When the value of D decreases further, the flexibility of the crack reduces. The straight and inflexible crack tends to break away from pinning positions, resulting in a reduction of G_{1c}. At $D^{-1} > 30\ mm^{-1}$ the linear relationship is not obeyed.

This does not imply that crack pinning does not occur at values of D less than 4×10^{-5} m. However, at high V_f, other effects such as the nucleation of microcracks at the carbon fibre poles, or the increase in brittleness of the matrix due to the constraint by neighbouring carbon fibres, become more important. This is supported by the following observations: (i) the "tails" and "steps" can be observed frequently in those specimens with D values larger than that at the maximum of the G_{1c} versus D^{-1} plot, but they are rarely found in the high V_f specimens and (ii) the stresses to nucleate the first crack, as indicated by the knee of the P–Δ curve, are lower in both specimens with $V_f = 0.25$ than those of the specimens with $V_f = 0.4$. Moreover, in the $V_f = 0.25$ specimens there was a considerable period of stable crack propagation before the maximum of the P–Δ curve was reached. This is probably due to the multiple bowing of crack segments.

The maximum pinning force $F_{max} = 2T$ calculated by using Equation 2 for the two SFRTPs are

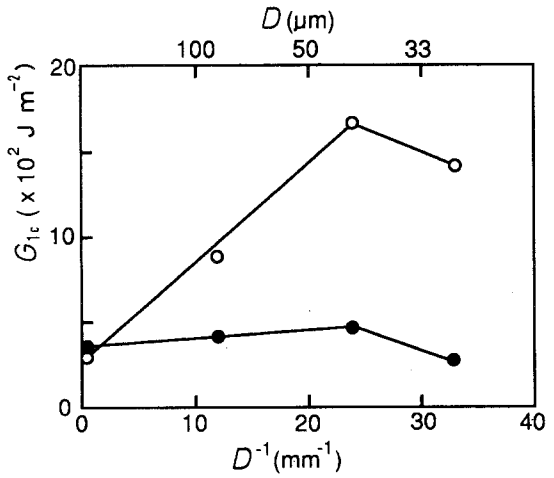

Figure 6 Plot of the fracture energy G_{1c} of the two SFRTP materials versus the reciprocal of the effective fibre spacing: (●) CF–PES-C, (○) CF–PPS.

4.2 kJ m^{-1} for CF–PES-C and 57 kJ m^{-1} for CF–PPS. The effective crack tension T is related to the energy per unit crack extension when the crack front is bowing. It is likely that the crack tension is primarily due to localized plastic deformation, with secondary contributions arising from debonding of the fibre–matrix interface and fibre pull-out.

It is also worth noting that the fracture energy of pure matrix PES-C is slightly larger than that of PPS. However, the toughening effect of carbon fibres on PPS is more marked. Moreover, the dynamic adhesive strength of the fibre–matrix interface in the CF–PPS composite is larger than that of CF–PES-C. Therefore, while the Young's moduli E of the two composites are the same, their values of strength σ_y and toughness, K_{1c} or G_{1c}, are different.

4. Conclusions

1. In the two SFRTP materials studied, the main energy-absorbing mechanisms during fracture are homogeneous and localized plastic deformation of the matrix, debonding of the fibre–matrix interface and fibre pull-out. The contribution of each mechanism depends on the match of strength and toughness between the fibre and the matrix, and the fibre–matrix adhesive strength.

2. The strength of the fibre–matrix interface is different under static and dynamic conditions. Static adhesion is concerned with the transferability of elastic strain or elastic stress by the interface before the initiation of cracking in the material, whereas dynamic adhesion is concerned with the transferability of plastic deformation by the interface while the material undergoes plastic deformation. The static bond strengths of the fibre–matrix interface in both CF–PES-C and CF–PPS composites are almost the same. However, their dynamic bond strengths are quite different.

3. The toughening mechanism in CF–PES-C and CF–PPS composites is essentially crack pinning in which the short carbon fibres play the role of pinning centres. The maximum pinning forces (i.e. effective crack tension) are 4.2 and 57 kJ m^{-1}, respectively. The fibre–matrix interface possesses medium bond strength and the main contribution to crack tension originates from localized plastic deformation of the matrix adjacent to the interface.

Acknowledgements

The authors are grateful to Dr Zhang Mingqiu of Zhongshan University, Guangzhou, China for the supply of the short carbon fibre reinforced composites, and to Mr Tan Shaohui and He Yuncai for carrying out the load–displacement tests.

References

1. A. C. MOLONEG, H.H. KAUSCH, T. KAISER and H. R. BEAR, *J. Mater. Sci.* **22** (1987) 381.
2. J. SPANOUDAKIS and R. J. YOUNG, *ibid.* **19** (1984) 473.
3. *Idem, ibid.* **19** (1984) 487.

4. R. J. YOUNG, in "Structure Adhesive", edited by A. J. Kinloch (Elsevier, London, 1986) Ch. 6.
5. N. AMDOUNI, H. SAUTEREAU. J. F. GERARD, F. FERNAGUT, G. COULON and J. M. LEFEBEVE, *J. Mater. Sci.* **25** (1990) 1435.
6. A. J. KINLOCH and R. J. YOUNG, in "Fracture Behaviour of Polymers" (Elsevier Applied Science, 1983) Ch. 11.
7. F. F. LANGE and K. C. RADFORD, *J. Mater Sci.* **6** (1971) 1197.
8. A. G. EVANS, *Phil. Mag.* **26** (1972) 1327.
9. D. J. GREEN, P. S. NICHOLSON and J. D. EMBERY, *J. Mater. Sci.* **14** (1979) 1657.
10. E. OROWAN, in Proceedings of Symposium on Internal Stress in Metals and Alloys (Institute of Metals, 1948) p. 451.
11. K. T. FABER and A. G. EVANS, *Acta Metall.* **31** (1983) 565.
12. S. YAMINI and R. J. YOUNG *J. Mater. Sci.* **15** (1980) 1823.
13. V. B. GUPTA, R. K. MITTAL and MALTI GOEL, *Compos. Sci. Technol.* **37** (1990) 353.
14. S. YAMINI and R. J. YOUNG, *J. Mater. Sci.* **15** (1980) 1814.
15. P. J. HINE, B. BREW, R. A. DUCKETT and I. M. WARD, *Compos. Sci. Technol.* **40** (1991) 47.
16. C. ZWEBEN, W. S. SMITH and M. W. WARDLE, in "Composite Materials: Testing and Design", edited by S. W. Tsai, ASTM STP674 (American Society for Testing and Materials, Philadelphia, 1979) p. 228.
17. H. KRENCHEL, "Fibre Reinforcement" (Akademisk Forlag, Copenhagen, 1964) p. 13.
18. M. J. FOLKS, "Short Fibre Reinforced Thermoplastics" (Research Studies Press, UK, 1985) p. 14.
19. D. C. PHILLIPS and B. HARRIS, in "Polymer Engineering Composites", edited by M. O. M. Richardson (Applied Science, 1977) p. 96.
20. C. K. Y. LEUNG and V. C. LI, *Composites* **21** (1990) 305.
21. T. RICCO, A. PAVAN and F. DANUSSO, *Polym. Engng Sci.* **18** (1978) 774.
22. D. B. MARSHALL and B. N. COX, *Acta Metall.* **33** (1985) 2013.
23. M. TAYA and R. J. ARSENAUIT, "Metal Matrix Composites" (Pergamon, UK, 1989) Ch. 3
24. G. L. HANNA and S. STEINGISER, in "Composite Materials: Testing and Design" edited by S. W. Tsai, ASTM STP674 (American Society for Testing and Materials, Philadelphia, 1979) p. 182.
25. L. M. MANOCHA, *J. Mater. Sci.* **17** (1982) 3039.
26. P. P. BANEAL and A. J. ARDELL, *Metallography* **5** (1972) 97.

Received 17 March 1992
and accepted 24 February 1993